

PAPER • OPEN ACCESS

Tropical forests are mainly unstratified especially in Amazonia and regions with lower fertility or higher temperatures

To cite this article: Christopher E Doughty *et al* 2023 *Environ. Res.: Ecology* **2** 035002

View the [article online](#) for updates and enhancements.

You may also like

- [Analyzing canopy height variations in secondary tropical forests of Malaysia using NASA GEDI](#)
E Adrah, W S Wan Mohd Jaafar, S Bajaj et al.
- [The use of GEDI canopy structure for explaining variation in tree species richness in natural forests](#)
Suzanne M Marselis, Petr Keil, Jonathan M Chase et al.
- [GEDI launches a new era of biomass inference from space](#)
Ralph Dubayah, John Armston, Sean P Healey et al.

ENVIRONMENTAL RESEARCH ECOLOGY



PAPER

OPEN ACCESS

RECEIVED
10 March 2023

REVISED
6 July 2023

ACCEPTED FOR PUBLICATION
13 July 2023



PUBLISHED
25 July 2023

Original content from
this work may be used
under the terms of the
[Creative Commons
Attribution 4.0 licence](#).

Any further distribution
of this work must
maintain attribution to
the author(s) and the title
of the work, journal
citation and DOI.



Tropical forests are mainly unstratified especially in Amazonia and regions with lower fertility or higher temperatures

Christopher E Doughty^{1,*} , Camille Gaillard¹ , Patrick Burns¹ , Jenna M Keany¹,
Andrew J Abraham¹ , Yadvinder Malhi², Jesus Aguirre-Gutierrez², George Koch³, Patrick Jantz¹ ,
Alexander Shenkin¹ and Hao Tang⁴ 

¹ School of Informatics, Computing, and Cyber Systems, Northern Arizona University, Flagstaff, AZ, United States of America

² Environmental Change Institute, School of Geography and the Environment, University of Oxford, Oxford, United Kingdom

³ Department of Biology, Northern Arizona University, Flagstaff, AZ, United States of America

⁴ Department of Geography, National University of Singapore, Singapore

* Author to whom any correspondence should be addressed.

E-mail: chris.doughty@nau.edu

Keywords: –GEDI, tropical forests, stratification, biomass

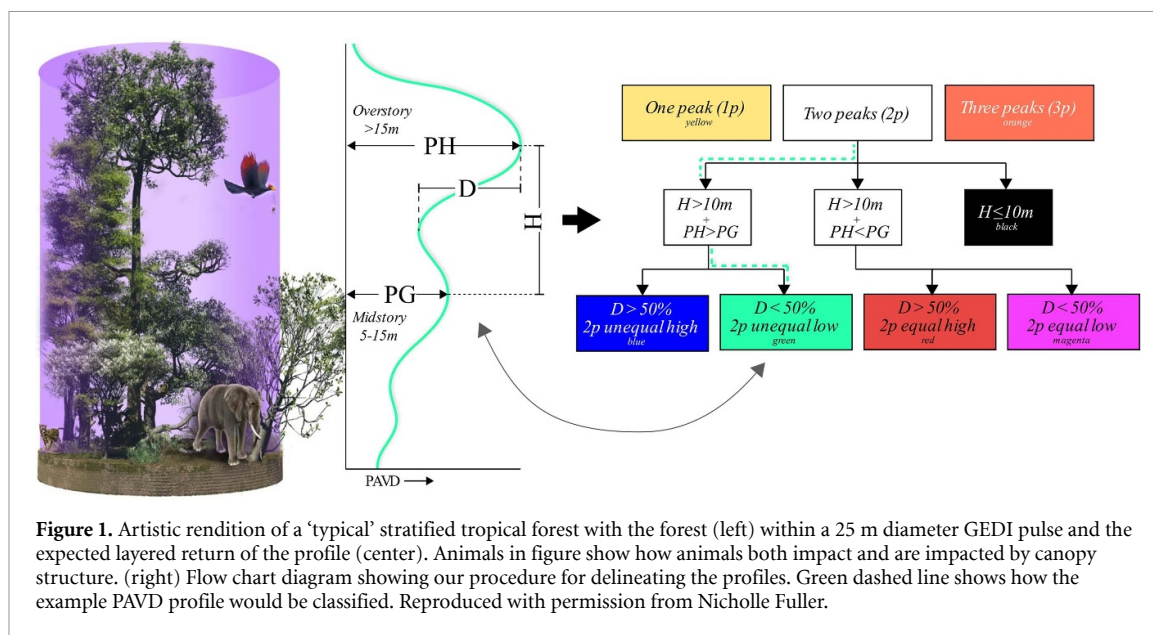
Supplementary material for this article is available [online](#)

Abstract

The stratified nature of tropical forest structure had been noted by early explorers, but until recent use of satellite-based LiDAR (GEDI, or Global Ecosystems Dynamics Investigation LiDAR), it was not possible to quantify stratification across all tropical forests. Understanding stratification is important because by some estimates, a majority of the world's species inhabit tropical forest canopies. Stratification can modify vertical microenvironment, and thus can affect a species' susceptibility to anthropogenic climate change. Here we find that, based on analyzing each GEDI 25 m diameter footprint in tropical forests (after screening for human impact), most footprints (60%–90%) do not have multiple layers of vegetation. The most common forest structure has a minimum plant area index (PAI) at ~40 m followed by an increase in PAI until ~15 m followed by a decline in PAI to the ground layer (described hereafter as a one peak footprint). There are large geographic patterns to forest structure within the Amazon basin (ranging between 60% and 90% one peak) and between the Amazon ($79 \pm 9\%$ sd) and SE Asia or Africa ($72 \pm 14\%$ v $73 \pm 11\%$). The number of canopy layers is significantly correlated with tree height ($r^2 = 0.12$) and forest biomass ($r^2 = 0.14$). Environmental variables such as maximum temperature (T_{\max}) ($r^2 = 0.05$), vapor pressure deficit (VPD) ($r^2 = 0.03$) and soil fertility proxies (e.g. total cation exchange capacity $-r^2 = 0.01$) were also statistically significant but less strongly correlated given the complex and heterogeneous local structural to regional climatic interactions. Certain boundaries, like the Pebas Formation and Ecoregions, clearly delineate continental scale structural changes. More broadly, deviation from more ideal conditions (e.g. lower fertility or higher temperatures) leads to shorter, less stratified forests with lower biomass.

1. Introduction

Early Western visitors describe tropical forests as *horror vacui* (nature abhorring a vacuum) since vegetation was 'anxious to fill every available space with stems and leaves', which was a change from more open temperate forests (Richards 1952). However, a closer examination of tropical forests revealed structure or stratification with 'a discernible, though complicated, arrangement in space' (Richards 1952). Halle *et al* (1980) built on this with their influential work identifying 23 unique tree architecture types and delving into the drivers of forest architecture (Halle *et al* 1980). They recognized that because tropical forests had fewer hydraulic or cold temperature constraints, the tropics was a good place to study the potential for trees to fill vertical space. They developed theories using detailed vertical profiles of 20 by 30 m old growth canopies



where ‘trees of the present’ occupy space in the upper canopy as well as in a second layer of increased light at 15–20 m where sunflecks converge. This old growth forest architecture would result in a stratified or layered forest (artistically rendered in figure 1) unlike younger pioneer forests with a single upper canopy stratum. We define a stratified or multilayer forest as having two or more peaks (or stratum = higher vegetation density) in horizontal vegetation (e.g. overstory and midstory in figure 1) with a lower amount of vegetation between them. Others have quantified stratification in different ways and found both temperate and tropical forests commonly have 2–3 tree layers or strata (Baker and Wilson 2000). However, tropical forest stratification has not been addressed previously at high spatial resolutions (e.g. 25 m diameter) at the pantropical scale.

More recently, the Global Ecosystems Dynamic Investigation (GEDI) on the International Space Station (ISS)-based LiDAR instrument (Dubayah *et al* 2020), allows us for the first time to peer into the structure of tropical forests in unprecedented resolution at a global scale. Prior to GEDI, there were other satellite lidar instruments (e.g. GLAS on ICESAT-1) used for measuring vegetation structure at large scale (Tang *et al* 2016, Tang and Dubayah 2017), but these were lower resolution, much more sparse, and focused on polar regions. At a more regional scale, aircraft and terrestrial lidar have shown detailed individual tropical forest tree architectures. For instance, aircraft lidar in tropical Peru found that tree architecture or shape (height of peak canopy volume (P) divided by canopy height) was highly correlated with canopy height (Asner *et al* 2014) and in Panama others successfully predicted the tree size distributions with airborne lidar (Taubert *et al* 2021). At a global scale, Ehbrecht *et al* (2021) used terrestrial laser scanning at a larger scale to show that forest structural complexity is a function of annual precipitation and precipitation seasonality (Ehbrecht *et al* 2021). Both simulation and sensitivity analysis suggest that high-quality GEDI data is able to provide measurements of similar accuracy for variables like plant area index (PAI) or species richness in the tropics when compared to aircraft and terrestrial lidar (Marselis *et al* 2018, 2020). These different lidar tools (that inform on structure from the individual tree to global scale) can help us to better understand how vertical layers are stratified across the tropical forests globally.

Tropical forest structure matters because it is indicative of use by dependent organisms: for example, tall canopies were a strong predictor of habitat use by Baldfaced saki monkeys (*Pithecia irrorata*) in the Peruvian Amazon (Palminteri and Peres 2012) and structure data are increasingly being used in species distribution models (Burns *et al* 2020). However, structure is understudied because detailed pan-tropical structural data did not exist prior to GEDI, and yet it is where the bulk of the world’s species exist (Stork 2018) including over 75% of all vertebrates and 60% of neotropical mammal species (Kays and Allison 2001). Stratification of forest vertical layers has been hypothesized to increase rates of pollination and dispersal, optimize light use, increase inter-canopy CO₂ concentrations, reduce leaf, fruit and flower predation, and increase forest structural integrity (Smith 1973). Overall, structure also creates the habitat for all other forest dwelling species (Terborgh 1992). For instance, figure one shows animals both impacting and being impacted by forest structure.

Further, understanding tropical forest structure can give us new insights into forest biomass, which is a primary goal of GEDI. Currently the L4A product for tropical forests uses relative height (RH) RH 98 and

RH 50 to predict a median above ground biomass density AGBD of 300 Mg Ha^{-1} for tropical forests ($0.66 r^2$ and root mean square error (RMSE) of 10.4) (Duncanson *et al* 2022). Ecological theory suggests that a stratified forest with more large emergent trees is indicative of an older forest (Halle *et al* 1980), which generally has higher biomass and carbon content. Therefore, incorporating canopy layers may improve prediction of tropical forest biomass. Trait theory suggests that canopy scale leaf traits may also be correlated with tree architecture (Violle *et al* 2007). For instance, plant leaf traits have been related to plot level architecture in the tropics and predicted with leaf spectral data (Doughty *et al* 2017). Remotely sensed canopy trait maps using Sentinel-2 for phosphorus, wood density and specific leaf area (SLA) among other traits for broad swaths of tropical forests (Aguirre-Gutiérrez *et al* 2021) and such optically derived leaf traits may be correlated with structure at the landscape scale.

Stratification of forest vertical layers may be due to genetic constraints that evolved over time (floristics) or trees not achieving their genetic heights (potential height under optimal environmental conditions). The debate about what sets the upper limits of tree height largely involves either hydraulic limitation (Koch *et al* 2004), mechanical limitation, or environmental factors such as wind speed (Jackson *et al* 2021). Certain factors drive heights such as the need to overtop competitors or disperse seeds while other factors reduce it such as hydraulic failure and vulnerability to wind. Environment alone could also directly impact tree height and structure, with hydraulic limitations, carbon deficiencies, or wind regimes causing trees to not being able to achieve their genetic height. There is a literature describing how the environment (soils or climate) impacts the species composition in tropical forests. For instance, Amazonian species composition may follow a south-west/north-east soil fertility gradient and a north-west/south-east precipitation gradient (ter Steege *et al* 2006). Soil cation concentrations are the primary driver of floristic variation for Amazonian trees (Tuomisto *et al* 2019) with climate being of secondary importance. However, in central African forests, climate is considered to be the driving factor of floristic patterns (Réjou-Méchain *et al* 2021).

The structure of forests is also a principal factor in determining not just the mean environment experienced by forest-dwelling organisms, but also the diversity, extent, and variability of microenvironments. The extent and diversity of microenvironments directly affects the niches available to organisms, and hence the diversity of forest-dwelling organisms. For instance, Oliveira and Scheffers (2019) proposed an ‘arboreality hypothesis’ where species have increased ranges because they can take advantage of changing microclimates in different canopy layers as temperatures shift due to elevation and latitude. They further suggested that future warming may push arboreal species towards the cooler ground layer (Oliveira and Scheffers 2019). Another study suggested that climate change may drive arboreal species in hot sparse canopies towards greater ground use (Eppley *et al* 2022). Detailed models now exist to predict canopy microclimate with forest structure as a possible input (Maclean and Klinges 2021). Therefore, forest structure can help determine microhabitats which becomes even more critical as climate change progresses.

Here we use GEDI to understand tropical forest structure and address the following questions:

Q1—Is the classic paradigm of ‘old growth’ tropical forest architecture with multiple canopy layers correct (visually represented in figure 1)?

Q2—What drives the geographic distribution of canopy structure (soils, e.g. total cation exchange capacity, environment, e.g. maximum temperature and/or leaf traits)?

2. Methods

2.1. GEDI data

We used the vertical forest structure (L2A and L2B, Version 2) and biomass (L4A—see below) products from the GEDI instrument (Dubayah *et al* 2020) based on the ISS between 18 April 2019 and 17 February 2021 for tropical forest regions (Amazonia, Central Africa, and SE Asia). The L2A product has already been ground validated in tropical forests and that is not a goal of this paper (Marselis *et al* 2018, 2020, Liu *et al* 2021, Cobb *et al* 2023). We principally used the plant area volume density (PAVD) profile, defined as the PAI (plant area index—which incorporates both leaf and wood) separated into 5 m vertical bins. We applied a number of data filters to ensure quality such as: degrade flag = 0 (e.g. not in degraded altitude), L2A and L2B quality flags = 1 (simplified metric to only use highest quality data based on energy, sensitivity, amplitude, and real-time surface tracking quality), sensitivity ≥ 0.95 , power beams during night and day and coverage beams during night only (nights are generally better to remove the negative impact of background solar illumination). To ensure that the footprints were in tropical forest regions, we applied three further data quality filters and two further data analysis filters.

2.2. Data quality filters

- (1) We used the well-established synthetic aperture radar dataset TanDEM-X (Krieger *et al* 2007) as a comparison to GEDI and removed GEDI data where elevation difference from GEDI is greater than ± 100 m indicating high uncertainty.
- (2) We used the well-established Landsat dataset to only include data with tree cover $>90\%$ in the year 2010, defined as canopy closure for all vegetation taller than 5 m (Hansen *et al* 2013).
- (3) We used the well-established MODIS dataset to further ensure that we select GEDI shot only in forest, by cross-validating forest cover with MODIS. The GEDI footprint was classified as plant functional type (PFT) Broadleaf Evergreen Tropical based on MODIS MCD12Q1v006 Product from 2021 (Friedl *et al* 2010) at 500 m spatial resolution following the Land Cover Type 5 Classification scheme. We identified the 25 m GEDI footprint within the 500 m MODIS pixel for comparison.

2.3. Data analysis filters

- (1) We screened out areas with tree heights <10 m using the RH metric 98% which was calculated as the height relative to ground elevation under which 98% percentage of waveform energy has been returned. To further ensure quality we vary this number in a sensitivity study (15, 20, and 25 m (figure S1)).
- (2) We compared an index of forest integrity as determined by degree of anthropogenic modification (Grantham *et al* 2020) to our results (figure S2).

If the L2a GEDI footprint passed these filters, we then estimated the number of canopy layers (peaks— P). If there were two layers, we estimated the height (H) and depth (D) differences between the two peaks (figure 1). Ecologically the number of peaks, as well as the height and depths between peaks will influence microclimate, vertical light environment, animal niche space, and biomass. In figure 1, we show an example GEDI footprint and then classify it using a flow diagram on the right.

- (1) We first classified each footprint by the number of local maxima (change in first derivative—hereafter: peaks = P) using the Matlab (Mathworks) function ‘islocalmax’ on each PAVD profile. If it had one peak, it was classified as one peak or stratum (yellow line figures 2 and 3). If it had two peaks, we further classified it (see below). If it had three or more peaks it was classified as 3 peak (orange line figures 2 and 3). We did not further classify waveforms with three or more peaks because they were rare ($<1\%$).
- (2) If the waveform had two distinct peaks, we then classified whether peak top (PT = the peak farther from the ground) had more PAVD than peak ground (PG = the peak closer to the ground). By distinct peaks we mean the peaks were more than 10 m vertically apart. If the peaks were not distinct (e.g. $H \leq 10$ m) then the peak was classified as 2p_even (black line figures 2 and 3).
- (3) We then used the following equation to determine if there was a large ($>50\%$) or small ($<50\%$) difference in the depth (D) of the peaks (where ABS is the absolute value):

$$D = \left(\text{ABS} \left(\frac{\text{PAVD of PT} - \text{PAVD of PG}}{\text{PAVD of PT}} \right) \right) * 100. \quad (1)$$

If $PG > PT$ with D less than 50% difference between the peaks, we classify it as 2p_eq_high (red line figures 2 and 3), if D is more than 50% difference it is classified as 2p_eq_low (magenta line figures 2 and 3). If $PG < PT$ with D less than 50% difference, it is classified as 2p_uneq_high (green line figures 2 and 3), if D is more than 50% difference 2p_uneq_low (blue line figures 2 and 3).

Overall, there are seven distinct profiles, but we do not show results from three plus peak forests as they were rare ($<1\%$). To calculate the percentage of one peak PAVD profiles (blue line figures 2 and 3), we sum the number of one peak profiles, divided by all profiles within a 0.1 by 0.1 degrees size grid cell (resolution was chosen for visual clarity). We recognize that our thresholds for H and D are somewhat arbitrary, and therefore, in a sensitivity study we tested these thresholds by changing H to 5 or 15 m and D to 40 or 60% but only found a change of $\sim 1\%$ in structural parameters on average (figure S3). The biggest change resulting in $\sim 2\%$ change in structural parameters occurred by increasing H to 15 m.

We downloaded the GEDI L4B AGBD product from DAAC (https://daac.ornl.gov/cgi-bin/dsvviewer.pl?ds_id=2017) and averaged it for each 0.1 by 0.1° pixel. With this data, we created a histogram of tree heights for each 0.1 by 0.1° subregion for all tree heights (RH 98) that pass our filters. The peak of the histogram is classified as median RH 98 tree height. For each 0.1 by 0.1° subregion, we estimate the total PAI as a proxy for commonly used metrics like leaf area index.

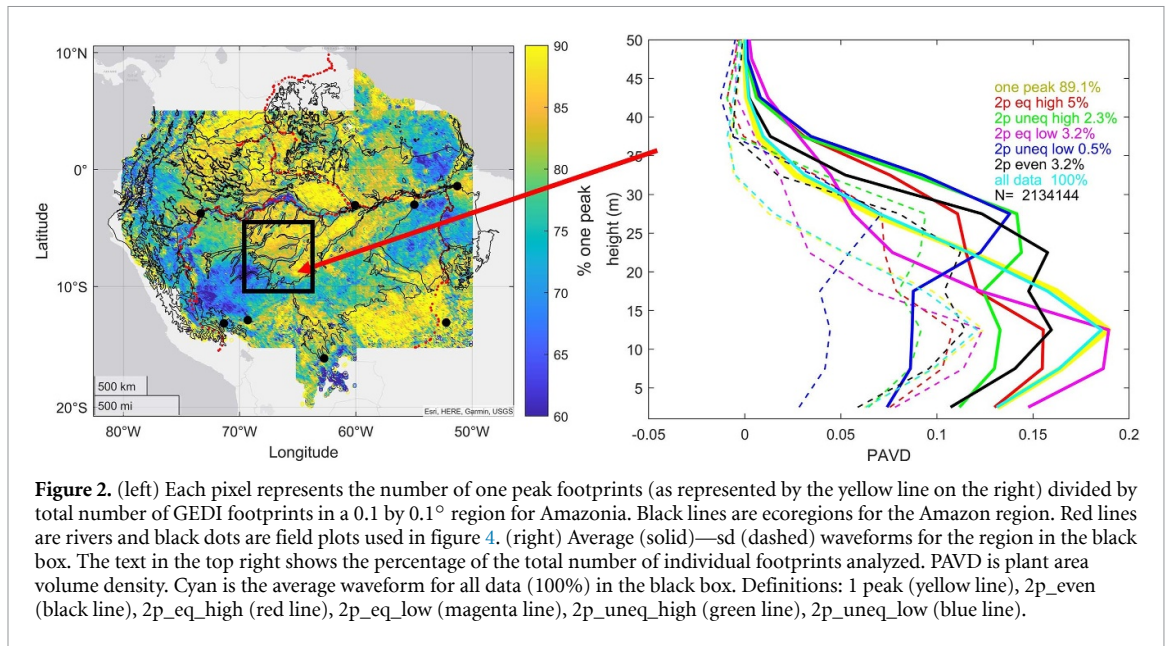


Figure 2. (left) Each pixel represents the number of one peak footprints (as represented by the yellow line on the right) divided by total number of GEDI footprints in a 0.1 by 0.1° region for Amazonia. Black lines are ecoregions for the Amazon region. Red lines are rivers and black dots are field plots used in figure 4. (right) Average (solid)—sd (dashed) waveforms for the region in the black box. The text in the top right shows the percentage of the total number of individual footprints analyzed. PAVD is plant area volume density. Cyan is the average waveform for all data (100%) in the black box. Definitions: 1 peak (yellow line), 2p_even (black line), 2p_eq_high (red line), 2p_eq_low (magenta line), 2p_uneq_high (green line), 2p_uneq_low (blue line).

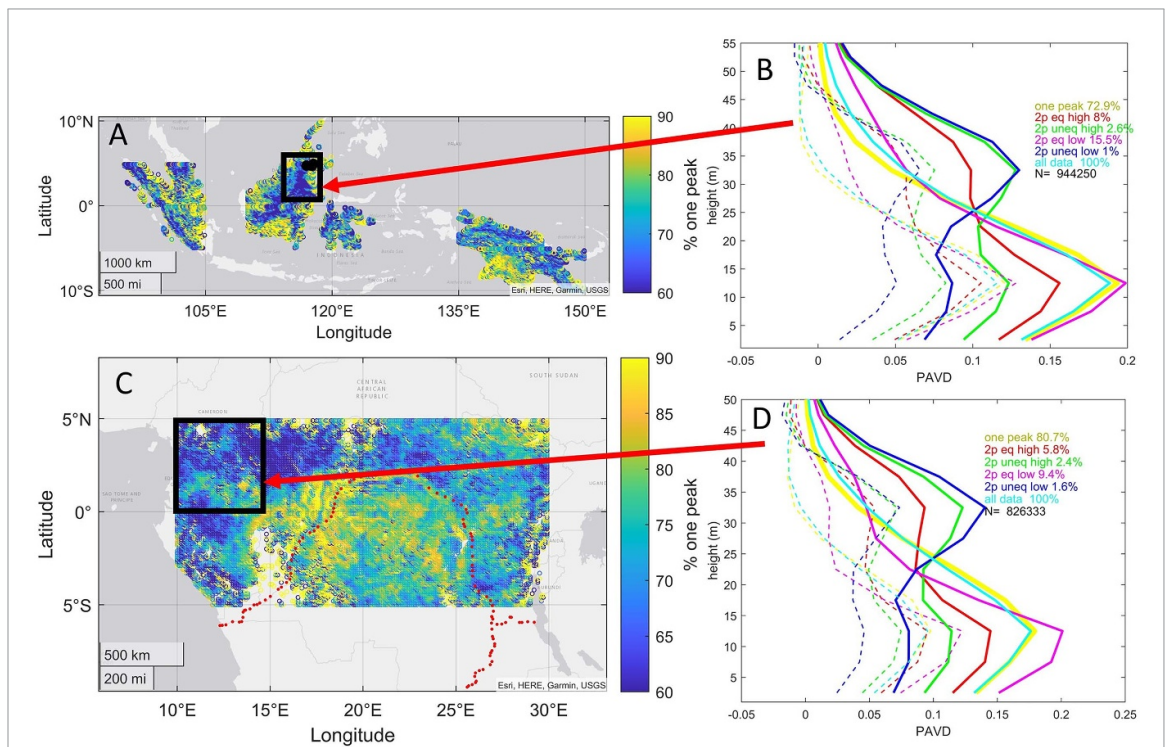


Figure 3. (left) Each pixel represents the number of one peak footprints divided by total GEDI footprints in a 0.1 by 0.1° region for SE Asia (A) and Central Africa (C). Red lines are major rivers. (right) Average (solid)—sd (dashed) vertical footprints for the region in the black box for SE Asia (B) and Central Africa (D). For each type, we give the percentage and the total number of individual footprints analyzed. Averages representing <1% were removed. PAVD is plant area volume density. Cyan is the average waveform for all data (100%) in the black box. Definitions: 1 peak (yellow line), 2p_eq_high (red line), 2p_eq_low (magenta line), 2p_uneq_high (green line), 2p_uneq_low (blue line).

2.4. Measuring scale dependence with individual tree data

We recognize that vertical canopy layers may be a function of spatial resolution. To test the dependence of vertical layers on spatial scale, we use a database (Araujo-Murakami *et al* 2014, Doughty *et al* 2015) where, for a series of plots in six diverse regions of the Amazon basin, we estimate stratification by calculating crown area using measured tree diameter at breast height (DBH) and tree height for individual trees in Caxiuana—4 ha, 2250 trees >10 cm DBH; Tambopata—2 ha, 1367 trees > 10 cm DBH; Iquitos—2 ha, 1165

trees > 10 cm DBH; Tapajos—18 ha, 1036 trees > 25 cm DBH; Bolivia—2 ha, 974 trees > 10 cm DBH; Tanguro—1 ha, 366 trees > 10 cm DBH. Plot locations are shown as black dots in figure 2. For each plot, we used tree height in each 5 m tree height bin (5–35 m) to estimate crown diameter following Asner *et al* 2002, shown below as equation (2), where DBH is the DBH (cm) and crown diameter is in meters,

$$\text{Crown diameter (m)} = 9.3 * \ln(\text{DBH (cm)}) - 22.2. \quad (2)$$

We estimate crown area to ground area ratio for all trees in the plots (e.g. Iquitos 2 ha = 1165 trees > 10 cm DBH) and on a subset of groups of 50 trees to better approximate the 25 m size of a GEDI footprint, as this is an approximate average number of trees >10 cm DBH per 25 m diameter circle in the tropics. For instance, a typical one hectare tropical forest plot would contain between 500 and 1000 trees with DBH > 10 cm (Malhi *et al* 2021) (~20 GEDI footprints if evenly spaced—which would not happen in practice) and each footprint, therefore, might contain 25–50 trees (with DBH > 10 cm). We then use the same ‘peak’ procedure (equation (1)) where we estimated the percentage of GEDI points with only one-peak for each region. We estimate crown area to ground area for each 5 m bin and vertically area summed. We also show median and maximum tree height for the plots. To test how the values in equation (2) influence our results, we varied the slope in equation (2) (9.3) by $\pm 5\%$ and show how this impacts the results in figure 4. To test the dependence of structure on spatial resolution, we estimate % one peak for spatial resolutions of 10 m (figure S4), 25 m and 1 ha (figure 4).

2.5. Comparison data layers

We compared percent one peak to several other climate, soils, leaf traits, and ecoregion maps listed below for the Amazon basin. Here we focus on the drivers of structure and validating GEDI for the Amazon region, but follow-on studies may do a similar analysis for Africa and SE Asia. Each dataset had its own resolution, which we standardized to 0.1 by 0.1°.

2.6. Soils

We used data from soilgrids www.soilgrids.org/ (Batjes *et al* 2020). We focused on total cation exchange capacity at pH 7 from 0 to 5 cm in units of mmol(c)/kg as previous studies had suggested this to be an important variable to explain floristic composition (Figueiredo *et al* 2018).

2.7. Climate

We averaged TerraClimate (Abatzoglou *et al* 2018) www.climatologylab.org/terraclimate.html data between 2000 and 2018 for climatic water deficit (CWD) (the difference between monthly reference evapotranspiration calculated using the Penman Monteith approach and actual evapotranspiration), VPD (VPD in kPa), mean monthly precipitation (mm/month), potential evapotranspiration (PET) and maximum and minimum temperature (°C). These data were originally based on climatic research unit time-series version 4 data and modified by Abatzoglou *et al* (2018).

2.8. Leaf traits

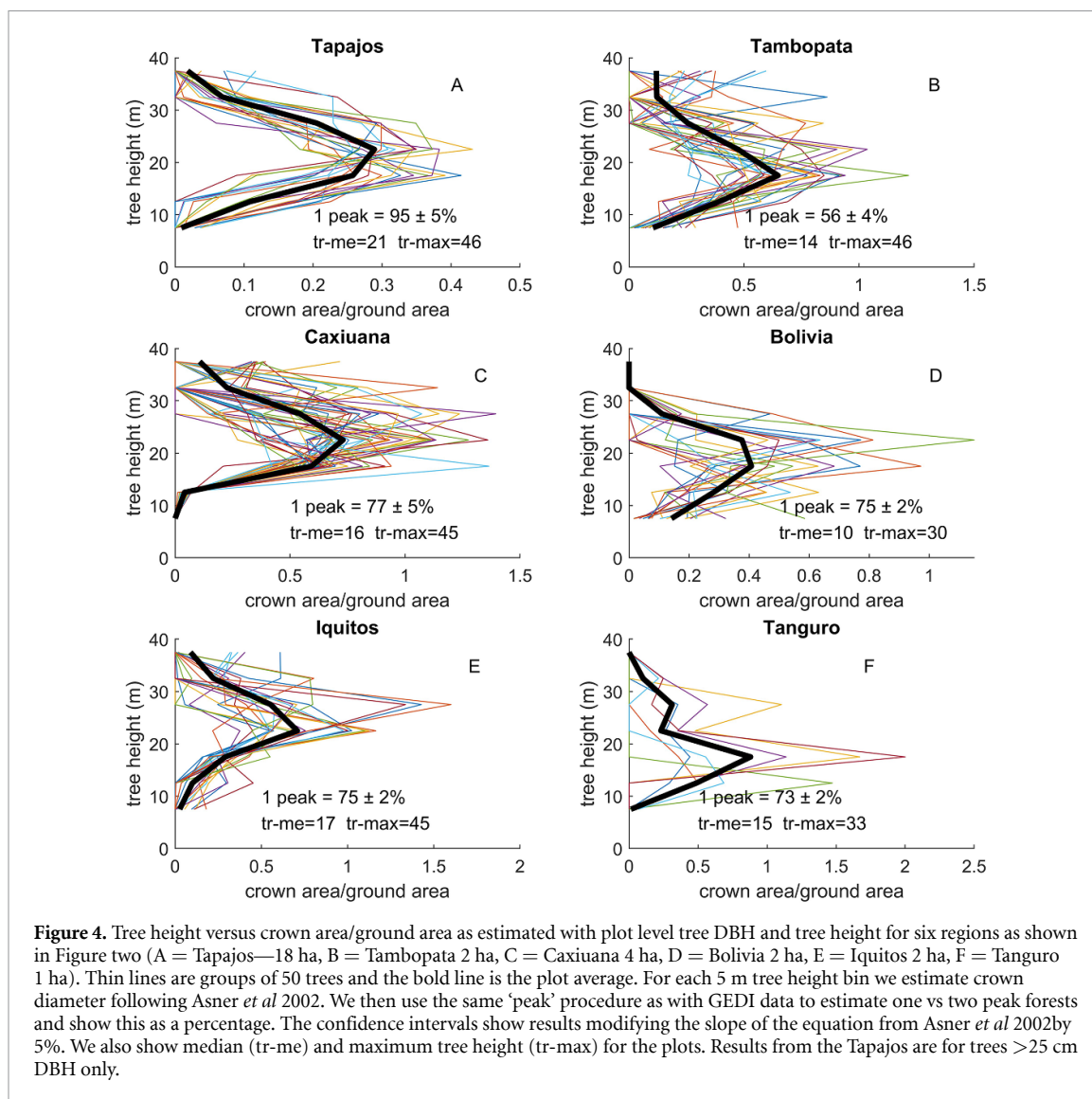
For plots in the Global Ecosystem Monitoring (GEM) network (listed in table 1) (Malhi *et al* 2021), we found the PAVD profile for the footprint closest to the plot as well as all footprints within a 0.03° grid around the plot coordinates. Most of these plots had *in situ* leaf traits measured to account for 70%–80% of the basal area (of trees >10 cm DBH) of 1 ha plots. Based on the field campaigns, (Aguirre-Gutiérrez *et al* 2021) used Sentinel-2 to create remotely sensed canopy trait maps for P = phosphorus %, WD = wood density g cm⁻³, and SLA = specific leaf area m² g⁻¹. We then compared the GEDI profile (% one peak) to the trait value predicted by those maps to that footprint.

2.9. Ecoregions

Ecoregions reflect the distributions of a broad range of fauna and flora across the entire planet and we use them as a proxy for plant biogeography www.sciencebase.gov/catalog/item/508fece8e4b0a1b43c29ca22—(Olson *et al* 2001).

2.10. Statistical analysis

We used the matlab function ‘fitlm’ to fit linear models and ‘fitnlm’ for the non-linear models to compare variables such as soils data, environmental data, or leaf trait data (at 0.1° resolution) to GEDI structure data of what percent of all footprints in a 0.1° area have one peak. The *P* values listed are for the *t*-statistic of the two-sided hypothesis test. We calculated the Beta weight (the regression slope) after standardizing both the dependent and predictor variables to *z*-scores using the matlab function *z* score.



3. Results

Most individual GEDI footprints in tropical forests do not have multiple layers (as artistically rendered in figure 1) and instead have a single peak in vegetation density at ~ 15 m, but this ranged geographically (regionally and between continents) between 60 and 90% (figures 2 and 3). Within the Amazon basin (figure 2), the broad geographic patterns were a large central region with low stratification, surrounded by another broad region with greater stratification bordered to the west by the Pebas formation (Higgins *et al* 2011), to the east by the Tapajos River, and the South at $\sim 12^\circ$ S. Another region of lower stratification occurred towards the southeast in the ‘arc of deforestation’ and savanna transition zones. River floodplains also tended towards increased stratification. The Congo basin showed a broadly similar spatial orientation with a central area with lower stratification surrounded by regions with greater stratification (figure 3). Southeast Asia, composed of mainly islands, showed greater stratification towards the island center (figure 3). The island of New Guinea had increasing stratification moving northward.

A low PAVD peak (e.g. ~ 15 m) may also indicate forest disturbance due to selective logging or other human impact. For instance, there was selective logging in parts of Borneo (Riutta *et al* 2018) and this impacted structure by increasing the dominance of shorter pioneer one-peak forests (i.e. Bornean logged plots (SAF table 1) are 78% one peak versus 44% for old growth forests) (table 1). However, the filters we used (tree height, MODIS PFT, logging product) should remove most human impact (although there may be older legacy effects we cannot account for). We tested this by increasing the minimum tree height (between

Table 1. Structure and trait data for regions surrounding plots from the GEM network (Malhi *et al* 2021). The columns are global region, RAINFOR plot code, plot structure classification for the footprint closest to the plot coordinates and the height of this footprint (highest vertical bin). Next is the average % one peak for footprints within 0.03° of the coordinates surrounding the plot and the average height of area. The last three columns are regionally averaged remotely sensed trait data (P = soil phosphorus %, WD = wood density g cm^{-3} , and SLA = specific leaf area— $\text{m}^2 \text{g}^{-1}$, Aguirre-Gutiérrez *et al* 2021).

Region	Rainfor code	Plot classification	Height	% 1 peak near plot	Average height	P	WD	SLA
SE Asia	DAN-04	Magenta	80	21	61	0.10	0.61	0.01
SE Asia	DAN-05	Yellow	35	22	60	0.10	0.61	0.01
SE Asia	LAM-01	Magenta	50	56	45	0.09	0.6	0.0105
SE Asia	LAM-02	Magenta	50	44	51	0.10	0.59	0.0104
SE Asia	MLA-01	Magenta	55	78	40	NaN	NaN	NaN
SE Asia	SAF-01	Yellow	45	88	43	0.10	0.58	0.0103
SE Asia	SAF-02	Yellow	40	71	44	0.10	0.59	0.0101
SE Asia	SAF-03	Yellow	40	80	44	0.10	0.58	0.0105
SE Asia	SAF-04	3-peak	95	53	62	0.10	0.6	0.0106
SE Asia	SAF-05	Yellow	35	100	38	0.10	0.58	0.0102
W. Amazon	ALP11	Blue	45	82	41	0.10	0.61	0.01
W. Amazon	ALP30	Yellow	40	80	41	0.10	0.6	0.01
W. Amazon	SPD02	Yellow	45	78	47	0.10	0.6	0.009
W. Amazon	SPD01	Yellow	60	80	46	0.10	0.6	0.0091
W. Amazon	TRU08	Yellow	40	81	47	0.10	0.6	0.0089
W. Amazon	TRU07	Yellow	50	79	49	0.10	0.6	0.0089
W. Amazon	ESP01	Yellow	40	88	38	0.12	0.62	0.0075
W. Amazon	WAY01	Yellow	45	87	43	0.12	0.62	0.0074
W. Amazon	TRU03	Yellow	50	98	38	0.11	0.62	0.0076
W. Amazon	ACJ01	Yellow	30	89	39	0.12	0.62	0.0078
E. Amazon	CAX-03	Yellow	40	82	38	0.09	0.61	0.0102
E. Amazon	CAX-06	Black	35	0	35	NaN	NaN	NaN
E. Amazon	STB-08	Yellow	45	69	45	0.09	0.61	0.0104
E. Amazon	STD-05	Yellow	40	81	35	0.08	0.65	0.0108
E. Amazon	STD-10	Yellow	40	94	38	0.09	0.62	0.0101
E. Amazon	STD-11	Yellow	30	85	39	0.08	0.61	0.0102
E. Amazon	STN-02	Blue	40	43	42	0.09	0.64	0.0104
E. Amazon	STN-04	Yellow	25	90	34	0.09	0.64	0.0103
E. Amazon	STN-06	Yellow	35	80	36	0.09	0.64	0.0102
E. Amazon	STN-09	Yellow	40	95	33	0.09	0.63	0.01
E. Amazon	STO-03	Yellow	45	70	44	0.08	0.66	0.0106
E. Amazon	STO-06	Yellow	35	89	44	0.08	0.65	0.0106
E. Amazon	STO-07	Yellow	40	73	44	0.08	0.66	0.0108
Gabon	IVI-01	Yellow	40	60	44	0.09	0.64	0.011
Gabon	IVI-02	Yellow	35	57	46	0.09	0.65	0.0109
Gabon	LPG-01	Black	45	57	44	NaN	NaN	NaN
Gabon	LPG-02	Yellow	50	33	56	NaN	NaN	NaN
Gabon	MNG-04	Yellow	25	63	42	NaN	NaN	NaN

15, 20 and 25 m) and found minor changes at the 25 m threshold, but no visible changes beyond that (figure S1). We also show comparisons of percentage of one peak to a forest disturbance product (Grantham *et al* 2020), which showed large regions dominated by one peak forests in areas of minimal human disturbance (figure S2).

On a subset of the Amazon (5 by 5° black box regions chosen to represent the broader region in figures 2 and 3), we averaged the vertical profile for each footprint in each of six structural categories (see methods) and found ‘one peak’ forests peaked in PAVD at 15 m with a fairly linear decline going upwards until ~ 40 m (figure 2 yellow line = mean – sd). The next most common profile type was 2p_eq_high (figure 2 red line = mean – sd) at $\sim 5\%$ of the results. Average forest height of this forest type exceeded the one peak forests with a maximum height at ~ 45 m versus 40 m. This forest type ranged between 1% and 10% of forest pixels and was more abundant in the Southeast and Northwest of the Amazon (figure 6—similar figure for Central Africa is figure S5 and SE Asia figure S6). The third most common forest structure at 3.2% was represented by the black line (2p_even). This forest type ranged between 1 and 5% across the Amazon and was widely dispersed throughout the Basin. The next most common 2-peak structure at $\sim 3.2\%$ was magenta (2p_eq_low). This had a similar distribution to the ‘red (2p_eq_high)’ line, but with an additional hotspot in the Southeast that was not present in the ‘red (2p_eq_high)’ (figure 6).

Table 2. Percent one peak forest of all GEDI footprints closest to the GEM plots and within a 0.03° radius around the plot coordinates. Same as results from table 1 but averaged (\pm sd) by continental region.

	W. Amazon	E. Amazon	Gabon	SE Asia
Nearest to plot	90%	85%	80%	50%
Within a 0.03° radius	$84 \pm 28\%$	$73 \pm 26\%$	$54 \pm 12\%$	$61 \pm 27\%$

3.1. Compare GEDI structure to predicted structure

To test the dependence of vertical layers on spatial scale, for six locations (shown as black dots in figure 2), we used DBH, tree height, and a canopy diameter model (Asner *et al* 2002) to estimate that total vertically summed crown area/ground area averaged $1.8 \text{ m}^2 \text{ m}^{-2}$ (0.96–2.3 min max). Averaging at the 1 ha scale for all trees >10 cm DBH (>25 cm for the Tapajos) in the plots (size ranging between 2 ha and 18 ha) showed a single peak that averaged 20 m (between 17.5 and 22.5 m) in crown area/ground area (thick lines in figure 4). This 20 m height may be taller than the GEDI mean of 15 m due to the absence of smaller 0–10 cm DBH trees measured at the plots. We then subsampled 50 trees from each plot (a better approximation for the GEDI footprint size) and more stratification resulted. For these subsets, we calculated one peak/all data and found a low in Tambopata (figure 4(b)) of 56% one peak to a high of 95% one peak in the Tapajos (figure 4(a)) with the other sites ranging from 73% to 77% one peak, which is a good approximation of percentage one-peak across the Amazon basin ($\sim 79\%$) (figure 2). If we average across the 6 sites at a spatial resolution of 25 m (like GEDI) we find 75% one peak, but if we reduce the resolution to 10 m, then % one peak drops to 65% (figure S4), so the spatial resolution of the footprint clearly matters for our question. The Tapajos results must be viewed with caution because only large trees (>25 cm DBH) were recorded, which led to a very high percentage of one peak (single stratum) forests. According to figure 2, Tambopata and the Tapajos are near transition zones of high and low % one peak forests while most other plots are in areas of high % one peak (figure 2). Therefore, spatial scale matters since averaging over a wider spatial area will mask individual tree structure.

3.2. How representative is the structure in plot networks compared to the broader Amazon?

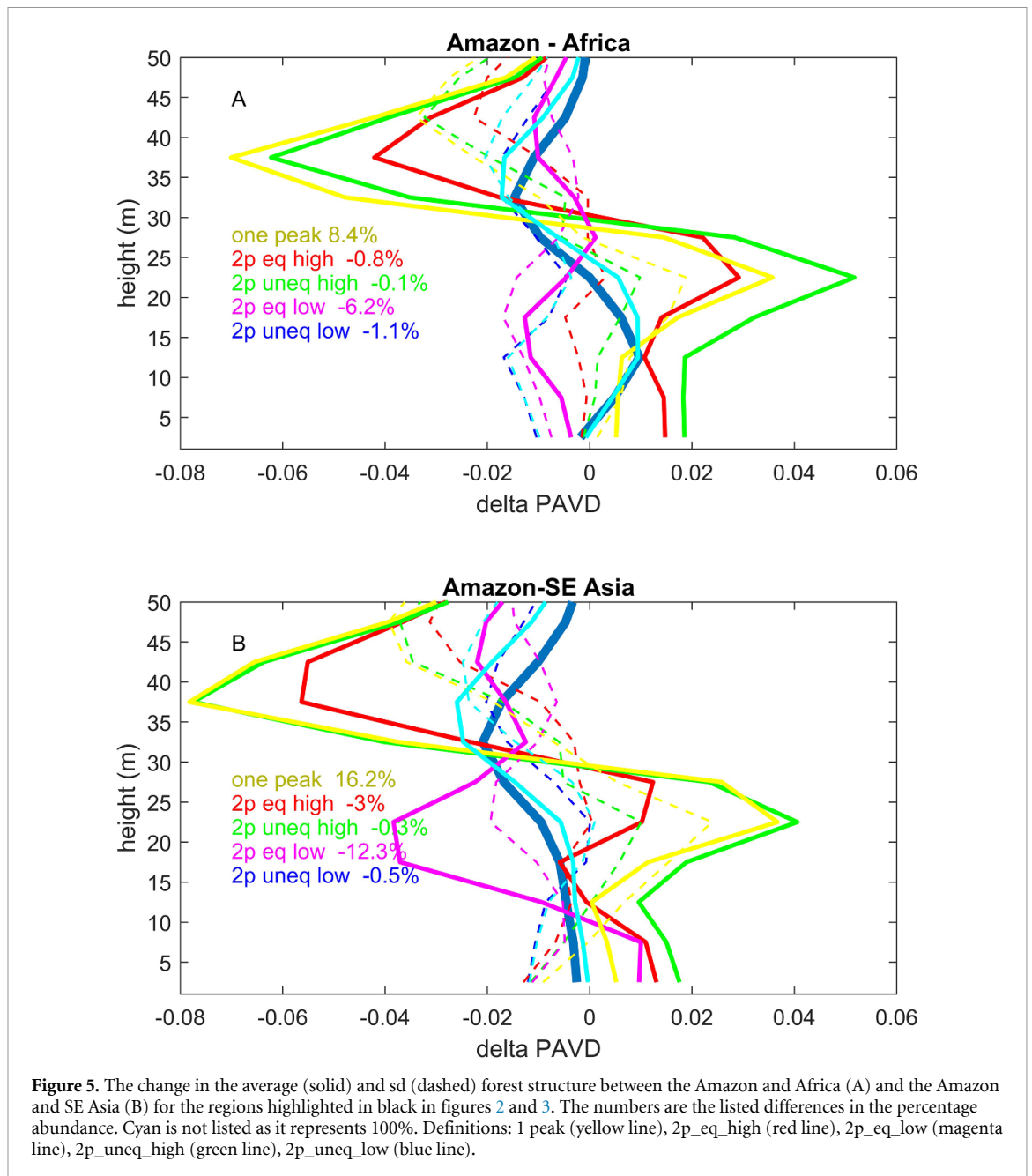
To answer this, we compare GEDI footprints (closest footprint and all footprints averaged within 0.03° radius of the plots) to a well-studied plot network (GEM—(Malhi *et al* 2021) in tables 1 and 2). We found the GEDI footprint nearest to the plots showed a gradient from the Western Amazon (90% one peak), Eastern Amazon (85%), Gabon (80%), to Borneo (50%). Averaging all nearby footprints showed similar, except for Gabon, but generally lower trends: Western Amazon (84%), Eastern Amazon (79%), Gabon (54%), and Borneo (61%). In table 1, we show data for each individual plot along with remotely sensed trait data (Aguirre-Gutiérrez *et al* 2021) calibrated from *in situ* measurements at the plot network. We found a significant relationship (figure S9) between structure and SLA ($r^2 = 0.12$, $P < 0.05$, % one peak = $-68 \cdot \text{SLA} + 1.4$) but not with wood density and percent phosphorus. However, this is a pan tropical analysis, and the signal is dependent on low SLA values along an elevation gradient where GEDI is less accurate because of difficulty in discerning the ground layer. In Borneo, the GEM plot network (Riutta *et al* 2018) is along a logging gradient with a clear change in structure (78% one peak for logged plots versus 44% one peak for old growth forests). We found a significant increase in SLA ($P < 0.05$) with disturbance and a close to significant increase in %P with disturbance ($P = 0.06$).

3.3. Continental comparison

We compared the average PAVD profiles from the entire Amazon to the average PAVD profiles for all SE Asia and Africa (average continental scale 0.1 by 0.1° pixels and not just the black boxes in figures 2 and 3). On average, the Amazon had a greater percent of one peak forests ($79 \pm 9\%$ sd) than either SE Asia or Africa ($72 \pm 14\%$ v $73 \pm 11\%$). Median tree height (RH 98) was lower in the Amazon at 25.6 m than in Africa at 28.5 m or SE Asia at 28.7 m. In the black box regions shown in figure 3 for Africa and SE Asia, one peak forests were most abundant ($\sim 70\%$) with a similar peak at 15 m (figure 5). In both the Africa and SE Asia subplots, both red (2p_eq_high) and magenta (2p_eq_low) structure types were much more common forest structures than in the Amazon, accounting for $>20\%$ of forest types vs $<10\%$ in the Amazon. The average curves changed shape with Amazon having more PAVD in the mid-canopy ~ 20 m and Africa and SE Asia having more PAVD in the upper canopy ~ 30 m. River basins throughout the tropics had similar structural properties.

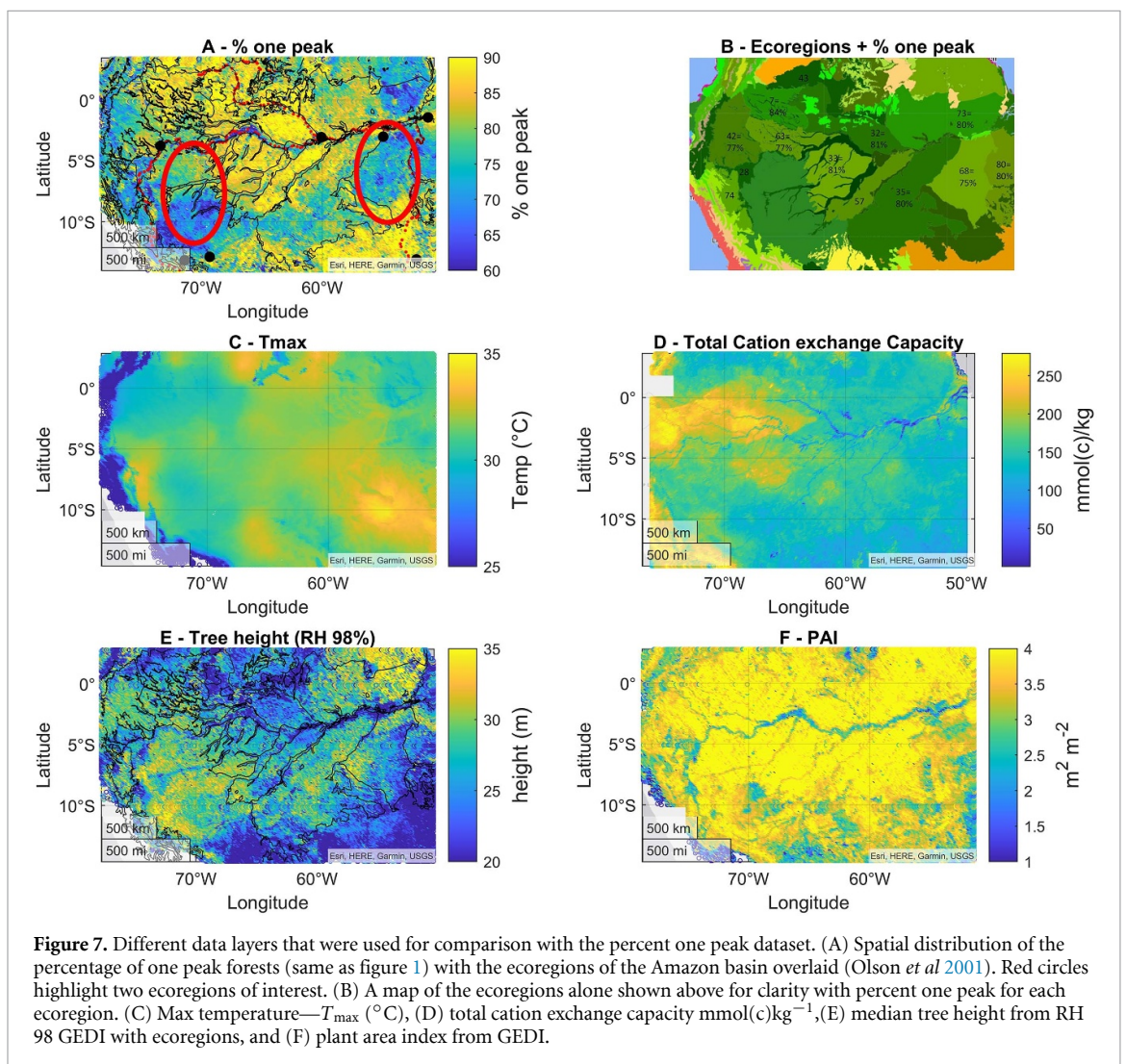
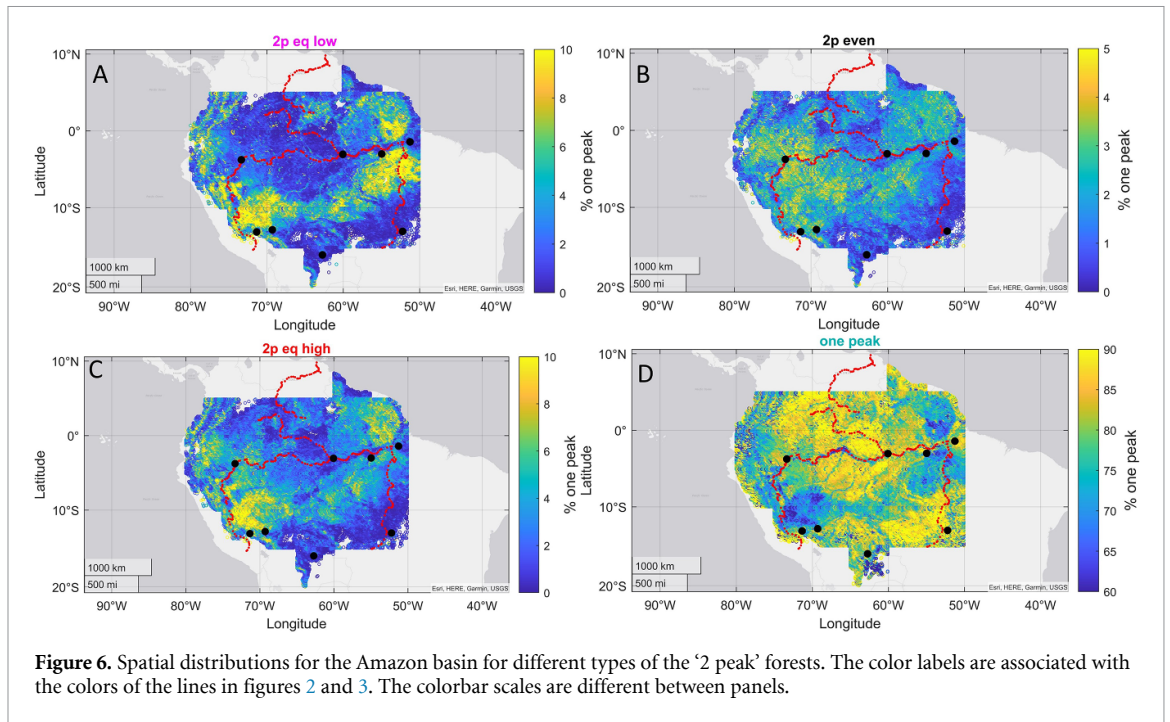
3.4. What controls structure?

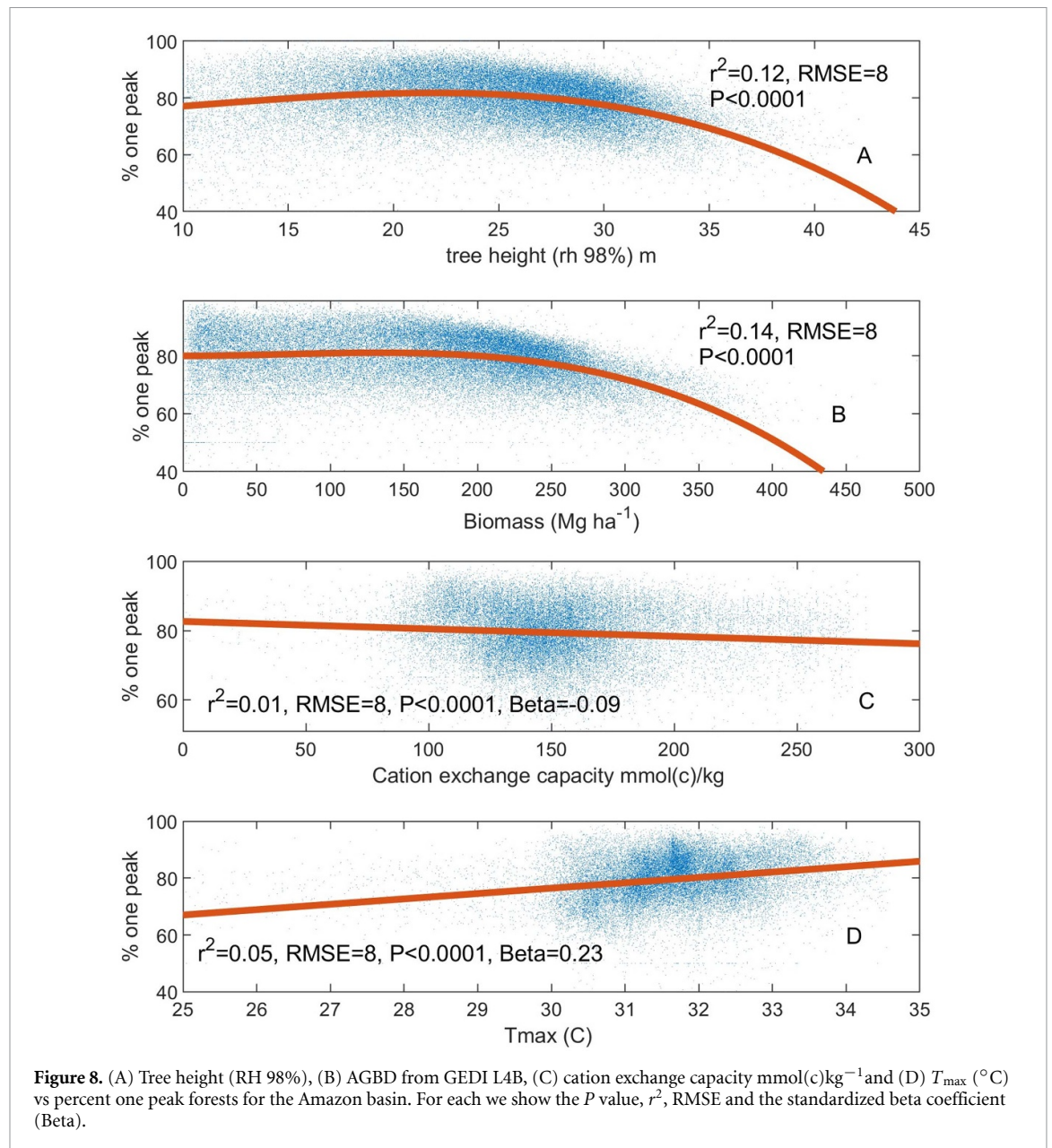
To explain the spatial patterns in the distributions of % one peak forests, we compared maps of percent one peak to a variety of datasets such as tree height (RH 98), ecoregions, GEDI L4A AGBD, PAI, number of



footprints, climate (VPD, PPT, CWD, PET, T_{\max} and T_{\min}), and total soils cation exchange capacity (figure 7—similar figure for Africa is figure S7 and SE Asia figure S8). The strongest correlations were with tree height and AGBD, with AGBD being a slightly better predictor for one peak forests (0.12 vs 0.14 r^2 respectively) (figure 8). We compared meteorological data for VPD, PPT, CWD, PET, T_{\max} and T_{\min} to percent one peak and all were highly significant ($P < 0.001$) but explained relatively little variance in the data. T_{\max} explained the most at 5% of the variance, followed by VPD at 2.5% and the others explaining $\sim 1\%$ of the variance. Likewise, total cation exchange capacity was highly significant but again explained only about 1% of the variation (figure 8). Other variables, such as number of footprints, were not related ($r^2 < 0.01$), but PAI explained $\sim 4\%$ of variance, which is again, likely related to tree height. We then combined all climate and soil variables which explained $\sim 9\%$ of variance and the key parameters were T_{\max} , VPD followed by total cation exchange capacity.

Ecoregions, which may be a good proxy for floristics, delineated structure well for particular ecoregions. For instance, ecoregion 68, the Tapajos-Xingu moist forest, (figures 7(a) and (b) right circle) had boundaries similar to boundaries of our structure dataset with a lower average value of percent one peak (75% vs 80%) than surrounding ecoregions. Another ecoregion, the southwest Amazon moist forest, with the boundary of the Pebas formation also delineated the structure data quite well. There were some regions that were partially





delineated well but not entirely. For instance, even ecoregion 68 (figures 7(a) and (b) left circle) had a sharp boundary in structure in the south not accounted for in the ecoregion.

4. Discussion

There are large ($>10\%$) differences in forest structure within the Amazon basin (60–90% one peak). Further, there are large average differences between the Amazon (79 ± 9 sd) vs. SE Asia and Africa (72 ± 14 v 73 ± 11 respectively). We are confident that the spatial patterns of structural changes are not mainly due to modern human influence, because we carefully screened for human influence using several independent remotely-sensed products (MODIS PFT) (Friedl *et al* 2010), a Landsat based deforestation product (Hansen *et al* 2013), and GEDI tree height itself (Dubayah *et al* 2020). Plot data from undisturbed regions (Doughty *et al* 2015) (DBH and tree height) showed similar structural trends in old growth plots (figure 4). Human influence, as measured through forest integrity (Grantham *et al* 2020), also did not explain our geographic patterns of structure (figure S2). The finding that the majority of GEDI footprints had a single PAI peak at ~ 15 m was initially surprising. However, several tropical aircraft lidar campaigns showed similar shape for the lowland tropics (a single peak when averaged over ~ 1 ha) but with a slightly higher peak in PAI at ~ 20 m (Asner *et al* 2014, Asner and Mascaro 2014). We hypothesize that the difference in the height of peak PAI may be due the difference in ‘energy return’ profiles. Due to an abundance of plant material in the lower canopy, it is necessary to correct for the reduced energy reaching the understory. Full waveform information

from GEDI can help correct for this energy return. In addition, prior work comparing TLS, LVIS and simulated GEDI data has found high-quality GEDI profiles on average to be accurate (Marselis *et al* 2018, 2020). Finally, we are confident that the bulk of structural differences across the tropics are of natural origin because on top of the filters applied, some regions of the Amazon far from human influence still had the dominance of one peak forests, such as the broad region north of Manaus in the Amazon, although there may be ancient legacy effects that we do not account for (figure S2).

The classic paradigm of ‘old growth’ tropical forest architecture (visually represented in figures 1 and figures in Halle *et al* 1980) is a generally closed upper canopy with large emergent trees at ~30–35 m where PAI peaks followed by a second peak at 15 m with slightly lower PAI. These PAI peaks at ~15 and 30 m are occupied by ‘trees of the present’ taking advantage of increased light cells (top of canopy and a second area of increased light at ~15 m where light flecks converge) (Halle *et al* 1980). This ‘classic paradigm’ implies a stratified canopy that might be best represented by the green (2p_uneq_low) or yellow (2p_uneq_high) lines in figures 2–5, but we find that this forest structure is relatively uncommon across the tropics making up just 3%–6% of tropical forest area. In contrast, by far the most common PAVD profile across the tropics has a single peak in PAI density at 15 m and this forest type likely reflects the absence of a closed upper canopy. In our color scheme (figures 2 and 3), we can think of a gradually increasing proportion of vegetation percent in the upper canopy going from the highest PAI at the top with blue (2p_uneq_high) (0.5% of total footprints), green (2p_uneq_low) (2%), red (2p_eq_high) (5%), magenta (2p_eq_low) (3%), and the lowest at yellow (1 peak) (86%). Overall, these results show that a ‘stratified’ forest with higher upper canopy closure is relatively rare across tropical forests.

Our structure maps broadly matched results from plot-based studies (figure 4). We also found strong correlations between our structure maps and detailed maps of structure, floristics, climate and soils for a broad region of Central Africa from Fayolle *et al* (2014) where old growth *celtis* forest is associated with regions with more vertical layers (~60% 1 peak) while more degraded or young *celtis* forests with more pioneer species is associated with less structure (70% one peak) (Fayolle *et al* 2014). A floristic map for all of central Africa also showed correlations with our structure map (Réjou-Méchain *et al* 2021) with, for instance, north (more structure) to south (less structure) gradients in Central Africa (figure 3) that match a transition in their figures from PCA 1, where floristics was controlled by a transition between cool, light-deficient forests and forests with high evapotranspiration rates, to PCA 2, where floristics were controlled more by seasonality and maximum temperature. In S.E. Asia, we compared our structure results to a logging gradient (Riutta *et al* 2018) with known structural changes and found GEDI footprints near Danum valley, where the tallest trees were found, also had some of the highest stratification (44% one peak) versus logged (78% one peak) which gives further confidence in the results. Broadly, old growth forests in SE Asia have the highest levels of stratification and this may be partially due to the presence of Dipterocarps which are the tallest tropical trees (Shenkin *et al* 2019, Jackson *et al* 2021).

Most of our independent datasets of soils or climate (as well as our combined model) did not strongly capture the spatial patterns of forest structure in the Amazon basin (figure 7). Tree height and AGBD did match these patterns (figure 8), but those variables cannot be considered independent of structure. However, patterns shown in figure 4(c) in Figueiredo *et al* (2018) are similar to the one we highlight in this study (figure 2) (Figueiredo *et al* 2018). Figueiredo *et al* (2018) created species distribution models for 40 species across the Amazon basin using 19 bioclimatic variables, 19 soil variables, and four remote sensing variables (including GLAS derived canopy height (Simard *et al* 2011)). Overall, for most species, a combination of soils and climate variables explain most variance (similar to (Tuomisto *et al* 2019)) but single-variable models did poorly with an average of less than 8% of the variance explained. This broadly reflects our attempts to model structure with single variables (given that the dependent variable is binary—i.e. one peak vs two—a lower r^2 is expected). There was a tight correlation between regions with less structure (e.g. higher percentage of one peak) and areas where soils are the limiting factor to species occurrence, and regions with greater structure (i.e. lower percentage of one peak) to areas where climate is the limiting factor to species occurrence. Perhaps deeper, more fertile soils allow for taller (either species or trees reaching their genetic height) and higher canopy closure forest types. Canopy height from the GLAS was the second most important variable for explaining species distributions, so it is possible that the Figueiredo *et al* (2018) map shows similar patterns to figure 2 due to the inclusion of the height metric (a strong predictor of structure). A global study of forest structure based on upscaling terrestrial lidar with WorldClim2 datasets showed some correlations with our structure maps but also missed many of the regional changes (Ehbrecht *et al* 2021).

Ecoregions delineated boundaries in structural composition in a few key areas of the Amazon basin like the Pebas formation (Higgins *et al* 2011) and the Tapajos region in Para, Brazil (figure 7). Higgins *et al* (2011) found a strong east-west gradient with an almost complete floristic turnover and an order of magnitude change in soil cation exchange capacity associated with the presence of the Pebas formation (Higgins *et al* 2011). The line marking the boundary of the Pebas formation also seems to strongly delineate

forest structure with one peak forests more abundant east of this line with lower cation exchange capacity and two peak forests more abundant to the west with higher cation exchange capacity. There is a further boundary delineated by the very wide (12–16 km) Tapajos River with forests to the west having a higher percentage one peak vs the eastern forests. Interestingly, some ecoregions (like 68) matched well with boundaries of vegetation structure, except for a few key areas (like in the south of region 68—figure 7). This may indicate that forest structure could be used in the future to improve upon current ecoregion boundaries.

4.1. What causes the dominance of one peak forests in the tropics and the spatial changes in these patterns?

A forest with a closed emergent canopy would have multiple stratum, but most forests likely lack a closed upper layer, leading to the dominance of the one peak forests. Rephrasing the initial question, we can instead ask: Is the rarity of a closed upper layer canopy (or relative rareness of large emergent trees) due to the environment (soils or climate) or floristics (species composition)? In practice it is difficult to disentangle floristics and environmental drivers and there is a large literature describing how the environment (soils or climate) impacts the species composition. For instance, Amazonian species composition may follow a south-west/north-east soil fertility gradient and a north-west/south-east precipitation gradient (ter Steege *et al* 2006). Soil cation concentrations is the primary driver of floristic variation for trees (Tuomisto *et al* 2019) with climate being of secondary importance at regional scales. Environment alone could also directly impact tree height and structure, with hydraulic limitations or nutrient deficiencies causing trees to not being able to achieve their genetic height. Soil depth can impact structure as shallow soils can cause stunted root growth leading to a thinner upper canopy structure (Halle *et al* 1980).

4.2. What may explain the continental scale differences in structure between the Amazon and other tropical regions?

Previous authors have noted large continental scale differences in AGBD and tree height (Borneo > Central Africa > Amazon) that broadly match the trends we show in structure (Feldpausch *et al* 2011, Lewis *et al* 2013). For instance, the Congo basin had average AGB values of 429 Mg ha⁻¹, similar to Bornean forests (445 Mg ha⁻¹), and much higher than the Amazon (289 Mg ha⁻¹) (Lewis *et al* 2013). We show similar broad trends with the Amazon at 79 ± 9 sd % one peak and 25.6 m height, SE Asia 72 ± 14 and 28.7 m height and Central Africa 73 ± 11 and 28.5 m (although these standard deviations overlap). Lewis *et al* (2013) had hypothesized that AGBD differences between Amazon and Africa were due to different biomass residence times and the differences between Africa—Borneo differences were possibly due to NPP differences. However, tree height and biomass are structural attributes and do not explain the difference in continental structure.

To fully understand structural gradients across the Amazon, higher resolution aircraft lidar can be used. Asner *et al* (2014) flew aircraft lidar along an elevation and nutrient gradient in Peru and found that canopy height and shape (height of peak canopy volume divided by canopy height) had a high, negative correlation with gap density (Asner *et al* 2014). Environmental stress either up an elevation gradient or from high soil fertility to low, led to shorter forests with more gaps and a peak canopy volume at a lower height in the canopy. These changes are broadly correlated with our maps of percentage of one peak, with perturbation (up elevation gradients or fertility gradients) increasing percentage of one peak forests. We found canopy stratification decreased as T_{\max} increased and soil fertility decreased (figure 8). Therefore, our results support this paradigm that moving away from ideal conditions may result in less structural complexity. Climate change will increase T_{\max} , but it is unclear whether this would further reduce structural complexity of tropical forests in the future.

In addition to tree height, remotely-sensed leaf traits were also related to structure near some of our plots. Increased stratification (lower percentage of one peak) was significantly correlated ($P < 0.05$) with increases in SLA (figure S9), but this was almost entirely driven by low SLA values in high elevation plots and removing these plots removed the significant correlation (Malhi *et al* 2021). Along a logging gradient in Borneo (Riutta *et al* 2018), less stratification as logging increased was significantly correlated with an increase in SLA and foliar concentrations of phosphorus, similar to other studies (Baraloto *et al* 2012) (Carreño-Rocabado *et al* 2016). However, Both *et al* (2019), also in Borneo, found a contrary result when comparing SLA along the forest gradient (Both *et al* 2019). Furthermore, Swinfield *et al* (2019) used high resolution aircraft hyperspectral data to predict SLA across the Bornean landscape (Swinfield *et al* 2019), but unlike most early studies (Doughty *et al* 2017) did not predict SLA accurately. Overall, we have reasons for caution for how well SLA can predict structure in tropical forests, but our abilities may improve in the future with hyperspectral satellites which could more accurately predict leaf traits at a global scale.

The primary goal of GEDI is to improve global predictions of biomass and incorporating structure could aid this goal. GEDI L4B was correlated ($r^2 = 0.12$ and 0.14) with both tree height (RH 98) and structure (%).

one peak). The GEDI algorithm uses tree height (RH 98) as a metric to predict biomass, and since tree height is correlated with structure, the similar strength of the correlations is not surprising (Duncanson *et al* 2022). However, there is a question of whether structure in addition to tree height can be used to improve biomass predictions. The dominance of one peak forests likely indicates more open upper canopy forests and Asner and Mascaro (2014) have shown these forest types make biomass prediction more challenging (Asner and Mascaro 2014). The plot data used to calibrate GEDI for tropical regions were not widely distributed throughout Amazonia, especially in the regions where height and structure diverge (figure 2). Understanding why height and structure diverge in these regions may be key towards understanding whether structure can improve biomass predictions in the future.

Overall, in most tropical forests, the upper canopy may be more open and stratification simpler than previously expected, and this has important implications for predicting biomass. Furthermore, our results indicate that tropical forest canopies may be more open than previously thought which may expose animals to greater climate change related heat stress and require modifications to their behavior (Oliveira and Scheffers 2019, Eppley *et al* 2022).

Data availability statement

The data and code that support the findings of this study are openly available at DOI: [10.5061/dryad.kd51c5bc4](https://doi.org/10.5061/dryad.kd51c5bc4) and the original GEDI data can be accessed at the following URL: https://lpdaac.usgs.gov/products/gedi02_av001/.

Acknowledgments

Support was provided by the GEDI mission and NASA Research Opportunities in Space and Earth Science Grants # 80NSSC20K0216, 80NSSC19K0206 and 80NSSC21K0191.

ORCID iDs

Christopher E Doughty  <https://orcid.org/0000-0003-3985-7960>

Camille Gaillard  <https://orcid.org/0000-0002-5184-5279>

Patrick Burns  <https://orcid.org/0000-0001-7971-4177>

Andrew J Abraham  <https://orcid.org/0000-0001-8625-8851>

Patrick Jantz  <https://orcid.org/0000-0001-5103-2270>

Hao Tang  <https://orcid.org/0000-0001-7935-5848>

References

- Abatzoglou J T, Dobrowski S Z, Parks S A and Hegewisch K C 2018 TerraClimate, a high-resolution global dataset of monthly climate and climatic water balance from 1958–2015 *Sci. Data* **5** 170191
- Aguirre-Gutiérrez J *et al* 2021 Pantropical modelling of canopy functional traits using Sentinel-2 remote sensing data *Remote Sens. Environ.* **252** 112122
- Araujo-Murakami A *et al* 2014 The productivity, allocation and cycling of carbon in forests at the dry margin of the Amazon forest in Bolivia *Plant Ecol. Divers.* **7** 55–69
- Asner G P, Anderson C B, Martin R E, Knapp D E, Tupayachi R, Sinca F and Malhi Y 2014 Landscape-scale changes in forest structure and functional traits along an Andes-to-Amazon elevation gradient *Biogeosciences* **11** 843–56
- Asner G P and Mascaro J 2014 Mapping tropical forest carbon: calibrating plot estimates to a simple LiDAR metric *Remote Sens. Environ.* **140** 614–24
- Asner G P, Palace M, Keller M, Pereira Jr, Rodrigo S, Jose N M and Zweede J C 2002 Estimating canopy structure in an Amazon forest from laser range finder and IKONOS satellite observations *Biotropica* **34** 483–92
- Baker P J and Wilson J S 2000 A quantitative technique for the identification of canopy stratification in tropical and temperate forests *For. Ecol. Manage.* **127** 77–86
- Baraloto C, Hérault B, Paine C E T, Massot H, Blanc L, Bonal D, Molino J-F, Nicolini E A and Sabatier D 2012 Contrasting taxonomic and functional responses of a tropical tree community to selective logging *J. Appl. Ecol.* **49** 861–70
- Batjes N H, Ribeiro E and van Oostrum A 2020 Standardised soil profile data to support global mapping and modelling (WoSIS snapshot 2019) *Earth Syst. Sci. Data* **12** 299–320
- Both S *et al* 2019 Logging and soil nutrients independently explain plant trait expression in tropical forests *New Phytol.* **221** 1853–65
- Burns P, Clark M, Salas L, Hancock S, Leland D, Jantz P, Dubayah R and Goetz S J 2020 Incorporating canopy structure from simulated GEDI lidar into bird species distribution models *Environ. Res. Lett.* **15** 095002
- Carreño-Rocabado G, Peña-Claros M, Bongers F, Díaz S, Quétier F, Chuvina J and Poorter L 2016 Land-use intensification effects on functional properties in tropical plant communities *Ecol. Appl.* **26** 174–89
- Cobb A R, Dommoin R, Sukri R S, Metali F, Bookhagen B, Harvey C F and Tang H 2023 Improved terrain estimation from spaceborne lidar in tropical peatlands using spatial filtering *Sci. Remote Sens.* **7** 100074
- Doughty C E *et al* 2015 Drought impact on forest carbon dynamics and fluxes in Amazonia *Nature* **519** 78–82

- Doughty C E *et al* 2017 Can leaf spectroscopy predict leaf and forest traits along a Peruvian tropical forest elevation gradient? *J. Geophys. Res.* **122** 2952–65
- Dubayah R *et al* 2020 The global ecosystem dynamics investigation: high-resolution laser ranging of the earth's forests and topography *Sci. Remote Sens.* **1** 100002
- Duncanson L *et al* 2022 Aboveground biomass density models for NASA's global ecosystem dynamics investigation (GEDI) lidar mission *Remote Sens. Environ.* **270** 112845
- Ehbrecht M *et al* 2021 Global patterns and climatic controls of forest structural complexity *Nat. Commun.* **12** 519
- Eppley T M *et al* 2022 Factors influencing terrestriality in primates of the Americas and Madagascar *Proc. Natl Acad. Sci.* **119** e2121105119
- Fayolle A, Picard N, Doucet J-L, Swaine M, Bayol N, Bénédict F and Gourlet-Fleury S 2014 A new insight in the structure, composition and functioning of central African moist forests *For. Ecol. Manage.* **329** 195–205
- Feldpausch T R *et al* 2011 Height-diameter allometry of tropical forest trees *Biogeosciences* **8** 1081–106
- Figueiredo F O G, Zuquim G, Tuomisto H, Moulatlet G M, Balslev H and Costa F R C 2018 Beyond climate control on species range: the importance of soil data to predict distribution of Amazonian plant species *J. Biogeogr.* **45** 190–200
- Friedl M, Sulla-Menashe D, Tan B, Schneider A, Ramankutty N, Sibley A and Huang X 2010 MODIS collection 5 global land cover: algorithm refinements and characterization of new datasets *Remote Sens. Environ.* **114** 168–82
- Grantham H S *et al* 2020 Anthropogenic modification of forests means only 40% of remaining forests have high ecosystem integrity *Nat. Commun.* **11** 5978
- Halle F, Oldeman R and Tomlinson P 1980 *Tropical Trees and Forests: An Architectural Analysis* (Springer)
- Hansen M C *et al* 2013 High-resolution global maps of 21st-century forest cover change *Science* **342** 850–3
- Higgins M A, Ruokolainen K, Tuomisto H, Llerena N, Cardenas G, Phillips O L, Vásquez R and Räsänen M 2011 Geological control of floristic composition in Amazonian forests *J. Biogeogr.* **38** 2136–49
- Jackson T D *et al* 2021 The mechanical stability of the world's tallest broadleaf trees *Biotropica* **53** 110–20
- Kays R, Allison A 2001 Arboreal tropical forest vertebrates: current knowledge and research trends BT—tropical forest canopies: ecology and management *Proc. ESF Conf. Oxford University (12–16 December 1998)* ed K E Linsenmair *et al* (Springer) pp 109–20
- Koch G, Sillett S and Jennings G 2004 The limits to tree height *Nature* **428** 851–4
- Krieger G, Moreira A, Fiedler H, Hajnsek I, Werner M, Younis M and Zink M 2007 TanDEM-X: a satellite formation for high-resolution SAR interferometry *IEEE Trans. Geosci. Remote Sens.* **45** 3317–41
- Lewis S L *et al* 2013 Above-ground biomass and structure of 260 African tropical forests *Phil. Trans. R. Soc. B* **368** 20120295
- Liu A, Cheng X and Chen Z 2021 Performance evaluation of GEDI and ICESat-2 laser altimeter data for terrain and canopy height retrievals *Remote Sens. Environ.* **264** 112571
- Maclean I M D and Klings D H 2021 Microclim: a mechanistic model of above, below and within-canopy microclimate *Ecol. Modelling* **451** 109567
- Malhi Y *et al* 2021 The global ecosystems monitoring network: monitoring ecosystem productivity and carbon cycling across the tropics *Biol. Conserv.* **253** 108889
- Marselis S M *et al* 2020 Evaluating the potential of full-waveform lidar for mapping pan-tropical tree species richness *Glob. Ecol. Biogeogr.* **29** 1799–816
- Marselis S M, Tang H, Armston J D, Calders K, Labrière N and Dubayah R 2018 Distinguishing vegetation types with airborne waveform lidar data in a tropical forest-savanna mosaic: a case study in Lopé National Park, Gabon *Remote Sens. Environ.* **216** 626–34
- Oliveira B F and Scheffers B R 2019 Vertical stratification influences global patterns of biodiversity *Ecography* **42** 249
- Olson D M *et al* 2001 Terrestrial Ecoregions of the World: a new map of life on earth: a new global map of terrestrial ecoregions provides an innovative tool for conserving biodiversity *BioScience* **51** 933–8
- Palminteri S and Peres C A 2012 Habitat selection and use of space by bald-faced sakis (*Pithecia irrorata*) in Southwestern Amazonia: lessons from a multiyear, multigroup study *Int. J. Primatol.* **33** 401–17
- Réjou-Méchain M *et al* 2021 Unveiling African rainforest composition and vulnerability to global change *Nature* **593** 90–94
- Richards P W 1952 *The Tropical Rain Forest* (Cambridge University Press)
- Riutta T *et al* 2018 Logging disturbance shifts net primary productivity and its allocation in Bornean tropical forests *Glob. Change Biol.* **24** 2913–28
- Shenkin A *et al* 2019 The World's tallest tropical tree in three dimensions *Front. For. Glob. Change* **2** 32
- Simard M, Pinto N, Fisher J B and Baccini A 2011 Mapping forest canopy height globally with spaceborne lidar *J. Geophys. Res.* **116** G04021
- Smith A P 1973 Stratification of temperature and tropical forests *Am. Nat.* **107** 671–83
- Stork N E 2018 How many species of insects and other terrestrial arthropods are there on earth? *Annu. Rev. Entomol. Ann. Rev.* **63** 31–45
- Swinfield T *et al* 2019 Imaging spectroscopy reveals the effects of topography and logging on the leaf chemistry of tropical forest canopy trees *Glob. Change Biol.* **26** 989–1002
- Tang H and Dubayah R 2017 Light-driven growth in Amazon evergreen forests explained by seasonal variations of vertical canopy structure *Proc. Natl Acad. Sci.* **114** 2640–4
- Tang H, Ganguly S, Zhang G, Hofton M A, Nelson R F and Dubayah R 2016 Characterizing leaf area index (LAI) and vertical foliage profile (VFP) over the United States *Biogeosciences* **13** 239–52
- Taubert F, Fischer R, Knapp N and Huth A 2021 Deriving tree size distributions of tropical forests from Lidar *Remote Sens.* **13** 131
- ter Steege H *et al* 2006 Continental-scale patterns of canopy tree composition and function across Amazonia *Nature* **443** 444–7
- Terborgh J 1992 Maintenance of diversity in tropical forests *Biotropica* **24** 283–92
- Tuomisto H, Van Doninck J, Ruokolainen K, Moulatlet G M, Figueiredo F O G, Sirén A, Cárdenas G, Lehtonen S and Zuquim G 2019 Discovering floristic and geoecological gradients across Amazonia *J. Biogeogr.* **46** 1734–48
- Vielle C, Navas M-L, Vile D, Kazakou E, Fortunel C, Hummel I and Garnier E 2007 Let the concept of trait be functional! *Oikos* **116** 882–92